A Theoretical Investigation of the Decomposition Mechanism of Pyridyl Radicals

Ruifeng Liu,* Thomas T.-S. Huang, James Tittle, and Daohong Xia†

Department of Chemistry, East Tennessee State University, Johnson City, Tennessee 37614-0695

Received: March 2, 2000; In Final Form: June 1, 2000

We carried out a detailed quantum mechanical study of the unimolecular decomposition mechanism of pyridine. The critical structures of all reasonable reaction pathways were optimized by density functional theory using the B3LYP functional and 6-31G** basis set. Relative energies were evaluated based on single-point QCISD-(T)/cc-pVDZ energies. In agreement with general belief and pervious theoretical studies, the calculated results indicate that C−H bond scission in pyridine preferentially produces the o-pyridyl radical. Also in agreement with the accepted mechanism, the calculations indicate that ring-opening via C−N bond cleavage in o-pyridyl radical is more favorable than C−C bond cleavage, as the former has a significantly lower activation barrier and the resulting open-chain cyano radical is more stable than other linear C_5NH_4 radicals. The calculated activation energy for the formation of cyanovinylacetylene + H from the open-chain cyano radical is the lowest, compared to the other channels considered. However, activation entropy favors C−C bond cleavage producing acetylene and cyanovinyl radical instead of cyanovinylacetylene and atomic hydrogen. On the basis of the calculated activation energies and activation entropies, transition state theory predicts that, in the temperature range of 1300−1800 K, the formation of acetylene + cyanovinyl radical from o-pyridyl radical is two to three times the rate of formation of cyanovinylacetylene + H. The calculations indicate that direct C−H bond scission from all three pyridyl radicals producing 2,3- and 3,4-pyridynes is also a favorable channel from energy consideration.

Introduction

Heavy fuels, such as coal and coal-derived liquids, are complex mixtures of aromatic hydrocarbons containing significant amounts of nitrogen and sulfur.[1] The combustion of them, used as an energy source in many power plants, produces oxides of these elements, which ultimately lead to environmental pollution.[2−4] Many strategies were developed to reduce the oxide formation, including the methods of deNO*x*[5] or RAPRENO*x*[6] as well as combustion modification techniques such as NO reburning, but a completely satisfactory solution has not been found. This is partly due to the fact that the complete combustion mechanism of heavy fuels is still unknown. It is known that fuel-bound nitrogen is mainly in the form of aromatic heterocycles such as pyrrole and pyridine rings.[1,7,8] The production of NO*x* in the combustion of heavy fuels is thought to occur through pyrolysis of volatilized fuel-bound nitrogen to form NO*x* precursors, which then react with oxygen to produce NO*x*.

Pyrrole and pyridine are ideal model compounds for studying the complex chemical reactions that occur when heavy fuels undergo pyrolysis and combustion. Thermal decomposition of pyrrole and pyridine has been the subject of many detailed experimental[9−13] and theoretical[14−18] investigations. It was reported that in the temperature range of 600−650 °C, the major products of pyridine decomposition are atomic hydrogen and 2,2′-bipyridine.[13] Hydrogen cyanide was observed at temperature above 650 °C, and complete cleavage of the pyridine ring was observed at 900 °C. A recent shock-tube pyrolysis study of Mackie et al. in the temperature range of 1300−1800 K found that in the low-temperature range, cyanoacetylene was the principal nitrogen-containing product.[11] At elevated temperature, hydrogen cyanide predominates. Other major products that are observed include acetylene and hydrogen. To explain the observed profiles of the major product species, Mackie et al. proposed the following mechanism as the main decomposition channel.

$$C_5H_5N\ (\text{pyridine}) \rightarrow o\text{-}C_5H_4N\ (\text{o-pyridyl}) + H$$

$$o\text{-}C_5H_4N\ (\text{o-pyridyl}) \rightarrow HC{=}CH{-}CH{=}CH{-}C{\equiv}N$$

$$HC{=}CH{-}CH{=}CH{-}C{\equiv}N \rightarrow HC{\equiv}CH + HC{=}CH{-}C{\equiv}N$$

$$HC{=}CH{-}C{\equiv}N\ (+M) \rightarrow HC{\equiv}C{-}C{\equiv}N + H\ (+M)$$

$$H + C_5H_5N\ (\text{pyridine}) \rightarrow o\text{-, m-, p-}C_5H_4N\ (\text{pyridyl}) + H_2$$

They also proposed some possible minor channels such as

$$HC{=}CH{-}CH{=}CH{-}C{\equiv}N \rightarrow HC{\equiv}C{-}CH{=}CH{-}C{\equiv}N\ (\text{cyanovinylacetylene}) + H$$

$$HC{=}CH{-}C{\equiv}N \rightarrow HC{\equiv}CH + C{\equiv}N$$

$$HC{=}CH{-}C{\equiv}N \rightarrow HC{\equiv}C + HC{\equiv}N$$

That is, the thermal decomposition is interpreted as a chain reaction initiated by C−H bond scission. Although a C−H bond scission in pyridine can lead to three unique pyridyl radicals, the o-pyridyl radical was favored by Mackie et al. because of its ability to produce an open-chain cyano radical directly, which is expected to be overwhelmingly more stable than any other open-chain radicals produced by the ring fissure of pyridyl radicals.

Mackie's mechanism of pyridine pyrolysis described above is well accepted and serves as an important reference for interpreting the pyrolysis reactions of many polycyclic aromatic compounds containing pyridine moiety.[19] However, because of the lack of reliable thermochemical data of many species

† On leave from the College of Chemistry and Chemical Engineering, University of Petroleum, Shandong, China 257062.

10.1021/jp000821q CCC: $19.00
Published on Web 08/18/2000

TABLE 1: Energies[a] of Pyridine, Pyridyl + H, and Pyridyne + 2H

method[b]	pyridine	o-pyridyl + H	m-pyridyl + H	p-pyridyl + H	2,3-pyridyne + 2H	3,4-pyridyne + 2H
B3LYP	−248.292 603	113.1	119.0	117.8	216.4	212.6
QCISD	−247.558 147	111.8	117.5	116.2	208.9	204.7
QCISD(T)	−247.594 749	111.1	116.9	115.7	205.5	199.7
ZPE[c]	55.8	47.7	47.6	47.4	39.8	39.9
QCISD(T) + ZPE[d]	0.0	103.1	108.7	107.4	189.5	183.8

[a] Total electronic energy of pyridine is given atomic unit (hartree); the energy of other species is given in kcal/mol relative to that of pyridine. [b] The 6-31G** basis set was used in the B3LYP calculations, and the cc-pVDZ basis set was used in all QCISD and QCISD(T) calculations. [c] Zero-point vibrational energy approximated by one-half of the sum of B3LYP/6-31G** harmonic vibrational frequencies. [d] QCIS(T)/cc-pVDZ energy with ZPE correction in kcal/mol relative to that of pyridine.

involved, arguments supporting the above mechanism were based on empirical estimates of many thermochemical data. To date, we are not aware of any detailed quantum mechanical study to examine validity of the mechanism.

Pyridine is isoelectronic with benzene. Mackie's decomposition mechanism of pyridine is also similar in many ways to the commonly assumed decylization/fragmentation mechanism of phenyl,[20−22] which is believed to lead to *n*-C_4H_3 and C_2H_2. A recent high-level quantum mechanical study[23] of unimolecular decomposition of phenyl radical by Lin et al. found, however, that when the temperature is below 1500 K, the dominant decomposition channel of phenyl is a C−H bond fissure producing o-benzyne and atomic hydrogen. When the temperature is above 1500 K, the formation of linear radicals becomes competitive with the cyclic isomer. However, the formation of the commonly assumed *n*-C_4H_3 + C_2H_2 was found to be less competitive than formation of *l*-C_6H_4 (1,5-hexadiyn-3-ene) and atomic hydrogen. These findings may have a significant impact on the interpretation of the pyrolysis processes of pyridine. We, therefore, decide to carry out a detailed theoretical study of the pyrolysis processes of pyridine.

Computational Details

All of the critical structures (equilibrium and transition states) along the proposed decomposition pathways were fully optimized by density functional theory using the B3LYP functional and the 6-31G** basis set. Vibrational analysis was carried out at the same level for each structure to make sure it had the desired number of imaginary vibrational frequencies. Intrinsic reaction coordinate analyses were performed at the B3LYP/6-31G** level on the transition structures to make sure that they led to the desired reactants and products. For a better estimate of relative energies, single point QCISD(T) calculations using the correlation consistent polarized valence double-ζ (cc-pVDZ) basis set were carried out on the structures optimized by B3LYP/6-31G**. Zero-point vibrational energy (ZPE) was taken into account and was approximated by one-half of the sum of B3LYP/6-31G** vibrational frequencies. For a reliable estimate of QCISD(T) energies, the cc-pVDZ does not appear to be an ideal basis set. We attempted QCISD(T) calculation with a larger basis set. However, open-shell UQCISD(T) calculation is very expensive. Our calculation with a larger basis set failed, due to inadequate computing resources. On the other hand, it has been shown that in similar studies,[24] QCISD(T)/cc-pVDZ calculation gives a reasonable estimate of energies. All of the calculations were carried out using the Gaussian94 program package.[25]

Results and Discussions

A. Stability of Pyridyl Radicals. Three unique pyridyl radicals can be produced via C−H bond scission in pyridine. An early semiempirical PRDDO (partial retention of diatomic differential overlap) calculation[17] and an ab initio molecular orbital study[18] indicated that the C−H bond ortho to the nitrogen atom is weaker than the other two C−H bonds. More recently, Jones et al. reported (RO)MP2/DZP energies of o-, p-, and m-pyridyl radicals.[26] Their results are in agreement with the semiempirical and early ab initio studies. However, their structures were optimized at ROHF/3-21G level of theory, which is known to be unreliable for many open-shell conjugated systems. In the present study, we calculated the structures and energies of all three pyridyl radicals. The formation of these radicals from pyridine via C−H bond scission is expected to have no reverse barrier. Our calculations indicate indeed that from pyridine to the pyridyl radicals, the energies increase monotonically with increasing C−H distance. The energies of pyridine, the three pyridyl radicals plus atomic hydrogen, and 2,3- and 3,4-pyridynes with two hydrogen atoms are presented in Table 1. In Table 1, the total electronic energy of pyridine is given in atomic units (hartree); the energies of the other species are given in kcal/mol relative to pyridine. It shows that in agreement with the early semiempirical and ab initio calculations, the o-pyridyl radical is about 6 and 4 kcal/mol more stable than the m- and p-pyridyl radicals, respectively. Compared to pyridine, the C−H scission products, o-pyridyl and atomic hydrogen, are 103 kcal/mol higher in energy (at the QCISD(T)/cc-pVDZ level with ZPE correction). In a shock-tube study, the rates of pyridine decomposition at temperatures between 1700 and 2000 K were measured, and a limiting high-pressure rate constant for pyridine disappearance, $k = 10^{16.2}\exp(-100$ kcal/mol/RT), was derived.[27] In the more detailed shock-tube pyrolysis study of Mackie et al.,[11] the rate constant of the principal initiation reaction, $C_5H_5N \rightarrow o\text{-}C_5H_4N + H$, was derived from fitting a 58-step reaction model and found to be $k = 10^{15.9\pm0.4}\exp(-98 \pm 3$ kcal/mol/RT). The activation energies derived from the two experimental studies are in good agreement with the calculated results. The rate constants derived from the latter shock tube study also implied an experimental heat of formation of o-pyridyl radical of $\Delta_f H° = 82 \pm 6$ kcal/mol and a heat of formation of $\Delta_f H° = 86 \pm 6$ kcal/mol for the m- and p-pyridyl radicals. The difference between the two agrees reasonably with our calculated relative energies between the o- and p-pyridyl radicals.

B. Decomposition Channels of the o-Pyridyl Radical. Several reasonable decomposition pathways of the o-pyridyl radical are described schematically in Figure 1, which shows that the pathway leading to o-pyridyne is very similar to the one from phenyl to benzyne in phenyl decomposition.[23] This pathway has been identified by Lin et al. as the most favorable pathway of phenyl decomposition. C−N bond cleavage in the o-pyridyl radical is considered more favorable than the C−C bond cleavage because the former leads to an open-chain cyano radical *l*-C_4H_3CN (**OE1** in Figure 1), whereas the open-chain radical generated by C−C bond cleavage (**OE5** in Figure 1) is expected to be less stable. C−H bond scission in **OE1** (via transition state **OTS4**) leading to cyanovinylacetylene (**OE4** in Figure 1) is very similar to the pathway from *l*-C_6H_5 to 1,5-

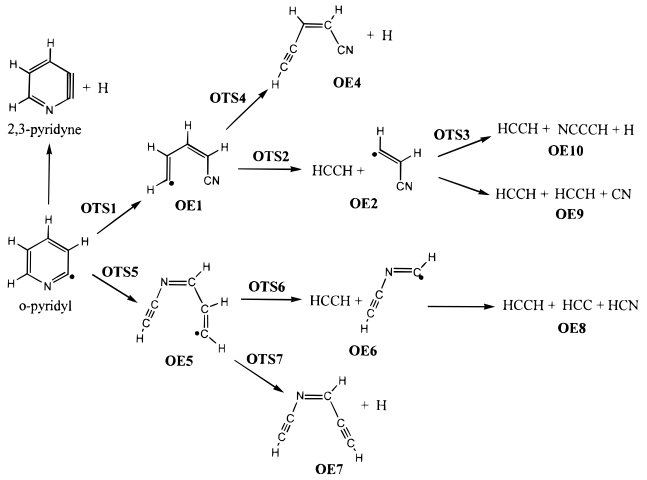

Figure 1. Unimolecular decomposition channels of o-pyridyl radical. Equilibrium structures are shown. Transition states are represented by the symbols above the arrows connecting the equilibrium structures.

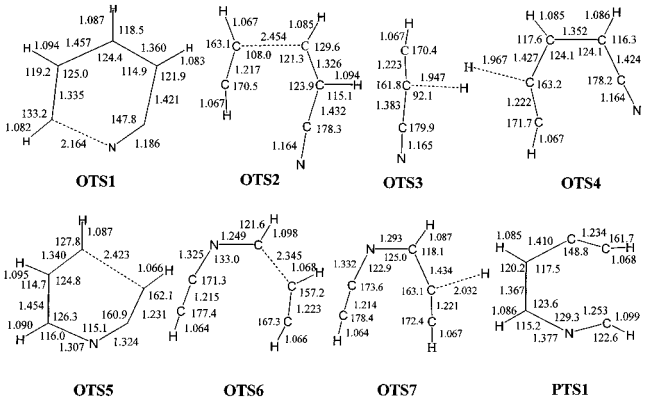

Figure 2. Prominent structural features of the transition states of unimolecular decomposition channels of o-pyridyl radical (Figure 1) and p-pyridyl radical (Figure 7) optimized by B3LYP/6-31G**. The bond distances are given in Å and angles in degrees.

hexadiyn-3-ene in phenyl decomposition, which Lin et al. found to be more competitive than formation of *n*-C_4H_3 + C_2H_2 (the equivalent of HC═CHCN (cyanovinyl radical) + C_2H_2, **OE2**, in pyridyl decomposition).

The structural features of the transition states described in Figure 1 optimized by B3LYP/6-31G** are presented schematically in Figure 2, which shows the bond lengths (given in Å) and bond angles (given in degrees). The energies of the structures described in Figure 1 were calculated relative to that of o-pyridyl radical from their B3LYP/6-31G**, QCISD/cc-pVDZ, and QCISD(T)/cc-pVDZ energies with ZPE correction. The results are presented in Table 2 in kcal/mol. The energies of 2,3- and 3,4-pyridynes are given in kcal/mol in Table 1 relative to that of pyridine. Much like the channel from phenyl to benzyne, our calculations indicate that there is no transition state for C−H bond cleavage in o-pyridyl yielding o-pyridyne. The products, o-pyridyne and atomic hydrogen, are 86.6 kcal/mol higher in energy than o-pyridyl radical.

The favored ring-opening transition state, **OTS1**, is predicted, at QCISD(T)/cc-pVDZ + ZPE level, to be 40.3 kcal/mol higher than the o-pyridyl radical and leads to the open-chain cyano radical **OE1**, which has a relative energy of 28.6 kcal/mol. From **OE1**, a C−C bond cleavage via **OTS2** leads to acetylene and cyanovinyl radical (**OE2**), which are 67.5 kcal/mol higher than the o-pyridyl radical. **OE2** decomposes further via C−H bond cleavage (**OTS3**) with an activation barrier of 110.2 kcal/mol to form cyanoacetylene and atomic hydrogen (**OE10**), or via a C−C bond cleavage to form a cyano radical and another acetylene (**OE9**). The C−C bond cleavage was found to have no transition state, the products are 118.2 kcal/mol higher in energy than o-pyridyl radical. **OTS4**, the transition state for C−H bond cleavage producing cyanovinylacetylene and atomic hydrogen (**OE4**), is predicted to have a relative energy of 68.5 kcal/mol. The products, **OE4**, have a relative energy of 59.2 kcal/mol.

Along the C−C bond cleavage pathway of o-pyridyl radical, the transition state **OTS5** is predicted to have a relative energy of 76.0 kcal/mol, which is nearly 36 kcal/mol higher than **OTS1**. The product, **OE5**, has a relative energy of 71.2 kcal/mol. In principle, **OE5** can further decompose via **OTS6** with a predicted activation energy of 106.3 kcal/mol, or via **OTS7** with a predicted activation energy of 112.7 kcal/mol.

The schematic energy profiles of the o-pyridyl decomposition pathways investigated in this study are presented in Figure 3. The energies in Figure 3 are those of QCISD(T)/cc-pVDZ with ZPE correction relative to that of the o-pyridyl radical in kcal/mol. It shows that the most energetically favorable decomposition pathway of the o-pyridyl radical is the one producing cyanovinylacetylene and atomic hydrogen. The highest activation barrier is 68.5 kcal/mol, and the products are 59.2 kcal/mol higher in energy than the o-pyridyl radical. C−H bond cleavage producing o-pyridyne is also a favorable channel. Although the energy of o-pyridyne and atomic hydrogen is higher than the ring-opening transition states **OTS2** and **OTS5**, subsequent fragmentation transition states and products along the **OTS2** and **OTS5** pathways are too high, compared to the two favorable channels. Overall, the results are very similar to those of phenyl decomposition, with the exception that in the latter, the most favorable channel is o-benzyne formation. The difference originates from the instability of o-pyridyne compared to o-benzyne as o-pyridyne is expected to be more strained due to the existence of a nitrogen atom in the ring.[28,29]

Table 2 and Figure 3 show that all of the small fragment products, HC≡CH + N≡C−C≡CH + H (**OE10**, 101.1 kcal/mol), HC≡CH + HC≡CH + CN (**OE9**, 118.2 kcal/mol), and HC≡CH + HC≡N, HC≡C (**OE8**, 125.7 kcal/mol), are very high in energy. Even the highest transition state leading to **OE10** (**OTS3**, 110.2 kcal/mol) is lower in energy than **OE9** and **OE8**. This indicates that acetylene and cyanoacetylene should be the major small fragment products, but at elevated temperatures,

TABLE 2: Relative Energies[a] of Critical Structures on the Decomposition Pathways[b] of the o-Pyridyl Radical

method	OTS1	OE1	OTS2	OE2	OTS3	OTS4	OE4	OTS5	OE5	OTS6	OE6	OTS7	OE7	OE8	OE9	OE10
B3LYP	47.8	37.8	87.2	86.7	135.1	84.8	82.0	80.3	76.0	117.5	98.9	125.5	123.5	158.1	151.5	130.9
QCISD	43.2	29.8	75.5	72.2	122.9	77.2	68.0	80.7	74.5	114.2	87.1	123.2	114.6	133.6	125.9	113.7
QCISD(T)	43.7	32.0	77.5	75.3	123.6	77.5	69.0	80.3	75.7	114.6	90.3	122.8	114.8	137.3	129.2	114.9
ZPE[c]	44.3	44.3	40.7	39.9	34.2	38.7	38.0	43.3	43.2	39.4	38.9	37.5	36.8	36.1	36.6	33.9
QCISD(T) + ZPE	40.3	28.6	70.5	67.5	109.4	68.5	59.2	76.0	71.2	106.3	82.0	112.7	104.0	125.7	118.2	101.1

[a] In kcal/mol relative to that of the o-pyridyl radical. The B3LYP calculations used the 6-31G** basis set; the QCISD and QCISD(T) calculations used the cc-pVDZ basis set. [b] The decomposition pathways are described in Figure 1. Prominent structural features of the transition states are given in Figure 2. [c] Zero-point vibrational energy approximated by one-half of the sum of B3LYP/6-31G** harmonic frequencies.

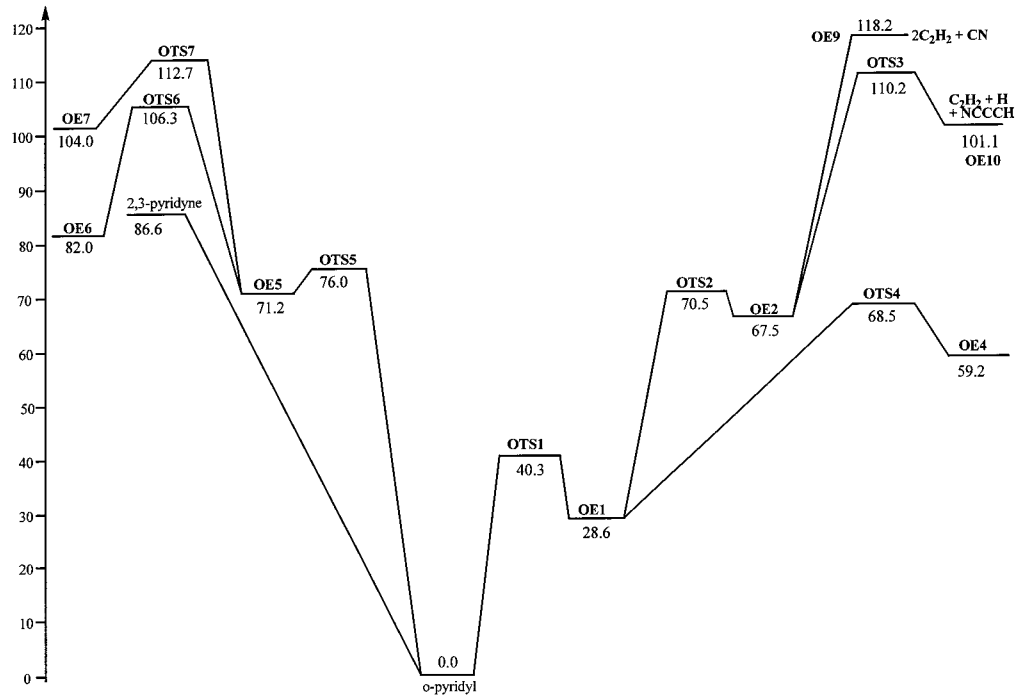

Figure 3. Energy profiles of unimolecular decomposition channels of o-pyridyl radical. The energies are given in kcal/mol relative to that of o-pyridyl radical, calculated from QCISD(T)/cc-pVDZ with zero point vibrational energy correction. The decomposition channels are described in Figure 1.

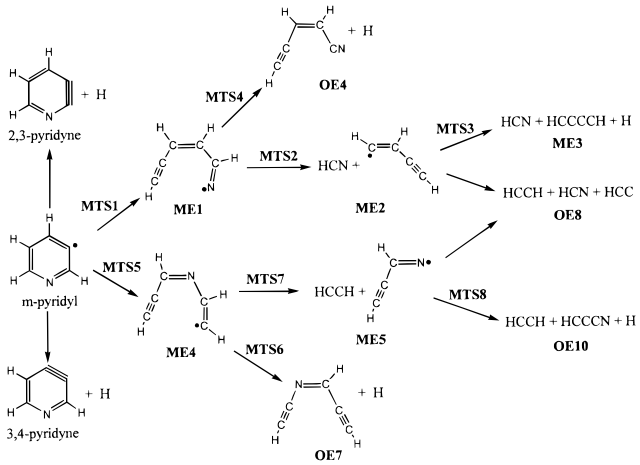

Figure 4. Unimolecular decomposition channels of m-pyridyl radical. Equilibrium structures are shown. Transition states are represented by the symbols above the arrows connecting the equilibrium structures.

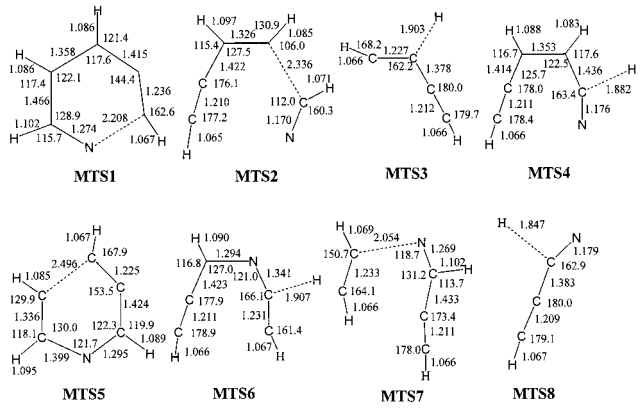

Figure 5. Prominent structural features of the transition states of unimolecular decomposition channels of m-pyridyl radical (Figure 4) optimized by B3LYP/6-31G**. Bond distances are given in Å, and Angles are given in degrees.

CN and HCN yield may increase. This is in agreement with the observation of Mackie et al.[11]

C. Decomposition Channels of the m-Pyridyl Radical. The decomposition channels of m-pyridyl radical investigated in this study are presented schematically in Figure 4. Two ring-opening channels were considered, one starts with C−C bond cleavage, the other starts with C−N bond cleavage. The structural parameters of important transition states optimized by B3LYP/6-31G** are presented in Figure 5. The energies of all of the structures in Figure 4 are given in Table 3 in kcal/mol relative to that of the o-pyridyl radical. For the m-pyridyl radical, C−H bond cleavage can lead to 2,3-pyridyne or 3,4-pyridyne. Much like the C−H bond cleavage in the o-pyridyl radical, no reverse barrier was found for C−H cleavage in the m-pyridyl radical producing 2,3- and 3,4-pyridyne. 3,4-pyridyne is predicted to be 5.7 kcal/mol lower in energy than 2,3-pyridyne.

Along the two ring-opening pathways, C−N bond cleavage via transition state **MTS1** leading to the open-chain radical **ME1** is more favorable than C−C bond cleavage via **MTS5** producing **ME4**. **MTS1** has a relative energy of 51.4 kcal/mol, whereas **MTS5** has a relative energy of 77.5 kcal/mol. In agreement with the discussion of Mackie et al., the open-chain radical **ME1** with a relative energy of 42.3 kcal/mol is 13.7 kcal/mol higher than the open-chain cyano radical **OE1**. At B3LYP/6-31G** + ZPE level of theory, **ME5** has a relative energy of 75.0 kcal/mol. Our QCISD(T)/cc-pVDZ calculation on **ME5** failed due to convergence problems in the SCF part.

Starting from **ME1**, C−C bond cleavage via **MTS2** (75.2 kcal/mol) generates **ME2** which has a relative energy of 67.9 kcal/mol. **ME2** can decompose further via **MTS3** (107.7 kcal/mol) into butadiyne, hydrogen cyanide, and atomic hydrogen (**ME3**, 98.1 kcal/mol), or dissociate via C−C bond cleavage without reverse barrier to produce acetylene, acetylyl radical, and hydrogen cyanide (**OE8**). However, the preferred decomposition pathway of **ME1** is C−H bond cleavage via **MTS4** to produce cyanovinylacetylene and atomic hydrogen (**OE4**). **MTS4**, the highest barrier for m-pyridyl → **OE4** along this

TABLE 3: Relative Energies[a] of Critical Structures on the Decomposition Pathways[b] of the m- and p-Pyridyl Radicals

method	MTS1	ME1	MTS2	ME2	MTS3	ME3	MTS4	MTS5	ME4[c]	MTS6	MTS7	ME5	MTS8	PTS1	PE1
B3LYP	57.3	48.8	91.0	86.6	131.4	126.9	86.2	83.8	79.6	127.8	107.3	98.9	137.0	70.6	60.5
QCISD	54.7	43.7	80.3	72.6	120.5	110.8	78.9	81.5		122.6	101.2	87.1	124.6	71.8	60.5
QCISD(T)	55.0	46.0	82.4	75.5	121.1	111.9	79.4	81.9		122.4	102.1	90.3	125.4	70.7	62.0
ZPE[d]	44.1	43.9	40.4	40.0	34.3	33.8	38.8	43.2	43.1	37.5	40.5	39.5	34.5	43.2	43.0
QCISD(T) + ZPE	51.4	42.3	75.2	67.9	107.7	98.1	70.5	77.5		112.3	94.9	82.1	112.3	66.2	57.3

[a] Energies are in kcal/mol relative to that of the o-pyridyl radical. The B3LYP calculations used the 6-31G** basis set; the QCISD and QCISD(T) calculations used the cc-pVDZ basis set. [b] The decomposition pathways are described in Figures 4 (m-pyridyl radical) and 6 (p-pyridyl radical). Prominent structural features of the transition states are given in Figure 5. [c] Attempts of QCISD(T)/cc-pVDZ calculations on this structure failed because of convergence problem in the SCF part. [d] Zero-point vibrational energy approximated by one-half of the sum of B3LYP/6-31G** harmonic frequencies.

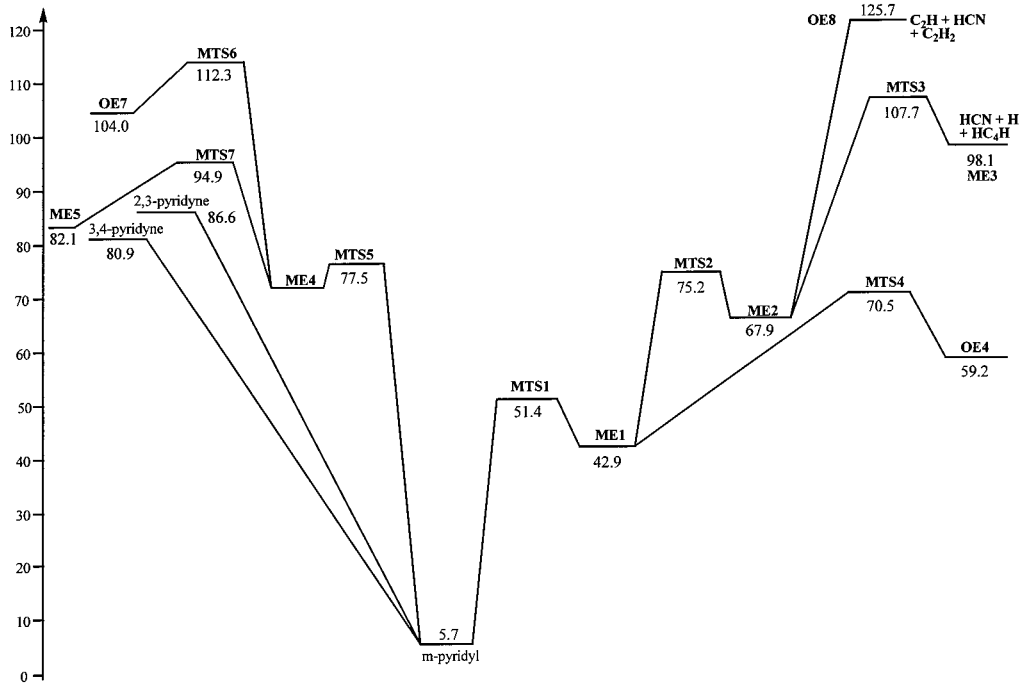

Figure 6. Energy profiles of unimolecular decomposition channels of m-pyridyl radical. The energies are given in kcal/mol relative to that of o-pyridyl radical, calculated from QCISD(T)/cc-pVDZ with zero point vibrational energy correction. The decomposition channels are described in Figure 4.

channel, has a relative energy of 70.5 kcal/mol, only 2 kcal/mol higher than the highest barrier for o-pyridyl → **OE4**.

ME4 has two reasonable decomposition channels: C−H bond cleavage via **MTS6** leading to **OE7** and C−C bond cleavage via **MTS7** producing **ME5**. Relative energies of **MTS6** and **MTS7** are predicted to be 112.3 and 94.9 kcal/mol, respectively. **ME5** also has two conceivable decomposition channels, a direct C−C bond cleavage without reverse barrier leading to **OE8** and C−H bond cleavage via transition state **MTS8** producing **OE10**. Schematic energy profiles of m-pyridyl radical decomposition are presented in Figure 6. It shows that the most energetically favorable pathway is again the one that leads to the formation of cyanovinylacetylene and acetylene. Much like o-pyridyl decomposition, C−H bond cleavage producing 2,3-pyridyne and 3,4-pyridyne is also more favorable than channels leading to small fragment products.

D. Decomposition Channels of the p-Pyridyl Radical. Only one reasonable ring-open channel of the p-pyridyl radical is conceivable, which is shown in Figure 6. The structural features of the ring-opening transition state, **PTS1**, are given in Figure 2 (see Figures 7 and 8). The relative energies of all the structures along this decomposition pathway are given in Table 3 in kcal/mol relative to that of the o-pyridyl radical. Similar to the o- and m-pyridyl radicals, a C−H bond cleavage in p-pyridyl radical leads to 3,4-pyridyne and atomic hydrogen with no reverse barrier. 3,4-pyridyne and atomic hydrogen is 80.9 kcal/mol higher than o-pyridyl radical.

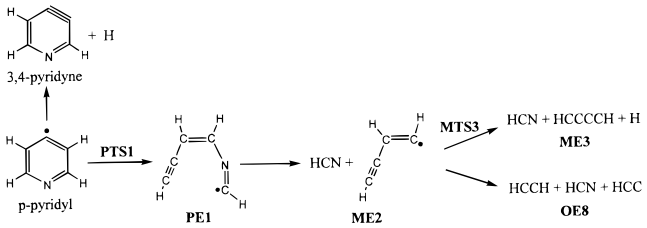

Figure 7. Unimolecular decomposition channels of p-pyridyl radical. Equilibrium structures are shown. Transition states are represented by the symbols above the arrows connecting the equilibrium structures.

Ring-opening in p-pyridyl radical via **PTS1** leads to an open-chain radical **PE1**, the relative energies of **PTS1** and **PE1** are 66.2 and 57.3 kcal/mol, respectively. A C−N bond cleavage in **PE1** leads to HCN and HC≡C−CH═CH (**ME2**) with no reverse barrier. **ME2** can further dissociate along the channels of the m-pyridyl radical.

E. Comparison with Experimental Results. The experimental studies indicated that under low temperature (600−900 °C) conditions, the thermal decomposition of pyridine resulted in atomic hydrogen and 2,2′-bipyridine.[13] This is consistent with the calculated results as the o-pyridyl radical is shown slightly more stable than the m- and p-pyridyl radicals. The combination

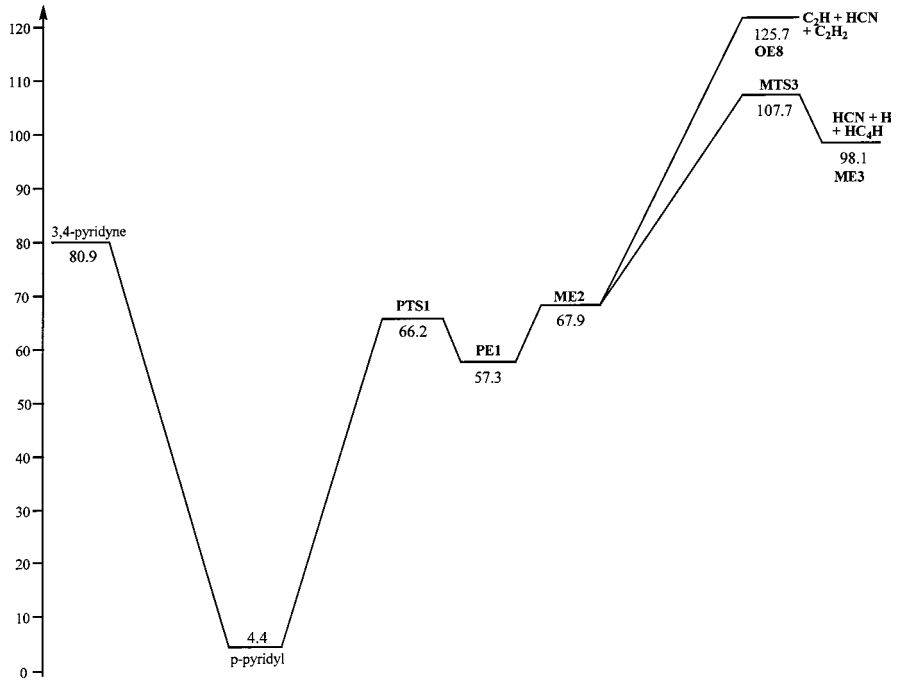

Figure 8. Energy profile of unimolecular decomposition channels of p-pyridyl radical. The energies are in given kcal/mol relative to that of o-pyridyl radical, calculated from QCISD(T)/cc-pVDZ with ZPE correction. The decomposition channels are described in Figure 7. Structural features of the transition state, **PTS1**, are given in Figure 2.

of two o-pyridyl radicals produces 2,2′-bipyridine. At elevated temperatures, atomic hydrogen, cyanoacetylene, hydrogen cyanide, and acetylene were observed as major decomposition products. However, the calculations indicate that for o- and m-pyridyl radicals, the most *energetically* favorable decomposition channels are those leading to the formation of cyanovinylacetylene. All of the unimolecular channels leading to the observed small-fragment products have very high activation barriers, even the products are much higher in energy. In their early experimental study, Mackie et al. could not positively identify cyanovinylacetylene as one of the products.[11] However, they did detect a likely cyano-containing product even at the lowest temperature at which decomposition could be observed. They tentatively assigned it to cyanovinylacetylene, but attempts to confirm it failed as the level of the product peak after transportation of the product gases for analysis dropped below sensitivity limits. They pointed out that cyanovinylacetylene is known to polymerize rapidly[30] above −30 °C. In their later related studies, they positively identified cyanovinylacetylene as a minor product of pyridine pyrolysis.[31,32]

Apart from the formation of cyanovinylacetylene, the calculations indicate that direct C−H bond cleavage of pyridyl radicals leading to the formation of 2,3- and 3,4-pyridynes is also an energetically favorable unimolecular channel. Much like the case of phenyl decomposition, pyridynes have not been observed in pyridine decomposition. However, it is well known that both benzyne and pyridyne are extremely unstable. It is likely that they react further immediately after they are produced. As the observed small-fragment products are much higher in energy than cyanovinylacetylene and pyridynes, they are very unfavorable products from energetic consideration alone. However, the rate of a chemical reaction depends on both activation energy and activation entropy. For the o-pyridyl radical, activation entropies of two crucial transition states, **OTS2** and **OTS4**, are predicted, from B3LYP/6-31G** harmonic vibrational frequencies, to be 16.02 and 12.74 cal·K^{-1}·mol^{-1}, respectively. The calculated activation energies of these two transition states are 70.5 and 68.5 kcal/mol (Table 2), respectively. Assuming first-order decomposition kinetics of **OE1** producing acetylene + cyanovinyl radical (via **OTS2**) and cyanovinylacetylene + H (via **OTS4**), transition state theory, $k = k_B T/h \exp(\Delta S^{\neq}/R + 1)\exp(-E_a/RT)$, predicts that the rate constant along **OTS2** is about twice the value of **OTS4** at the low-temperature end (1300 K) of the Mackie's experiment[11] and three times the value of **OTS4** at the high-temperature end (1800 K). Therefore, even though the energy of cyanovinylacetylene + H is the lowest among the observed products, in the temperature range of the experimental study, formation of acetylene + cyanovinyl radical is faster due to favorable activation entropy. In low concentration conditions, the chance of recombination between acetylene and cyanovinyl radical to reproduce **OE1** is low, and the likely fate of cyanovinyl radical is to decompose further producing smaller fragment products. Thus, the calculated results is in agreement with the experimental findings of Mackie et al.

Concluding Remarks

The results of our detailed theoretical calculations indicate that the most energetically favorable unimolecular decomposition channel of pyridyl radicals is ring-opening via C−N bond cleavage to form an open-chain cyano radical, followed by C−H bond cleavage leading to the formation of cyanovinylacetylene and atomic hydrogen. Much like the formation of benzyne in phenyl radical decomposition, C−H bond cleavage of pyridyl radicals leading to the formation of 2,3- and 3,4-pyridyne and atomic hydrogen is also a favorable unimolecular decomposition channel. However, when activation entropies are taken into consideration, the most kinetically favorable pyrolysis pathway of pyridine is C−H bond fission producing o-pyridyl radical, followed by C−C bond fission producing acetylene and cyanovinyl radical; the cyanovinyl radical may decompose further to generate smaller fragment products. This is in agreement with the experimental observations of Mackie et al. and supporting their conclusion.

Acknowledgment. This study was partially supported by the Petroleum Research Fund administrated by the American

Chemical Society and by a Cottrel College Science Award of Research Corporation.

References and Notes

(1) Unsworth, J. F. In *Coal Quality and Combustion Performance*; Unsworth, J. F., Barrat, D. J., Robert, P. T., Eds.; Elsevier Science Publishers: Amsterdam, 1991.

(2) Pershing, D. W.; Wendt, J. O. L. *16th Symp. (Int.) Combust. Proc.*; The Combustion Institute: Pittsburgh, PA, 1977; p 389.

(3) Painter, P. C.; Coleman, M. M. *Fuel* **1979**, *58*, 301.

(4) Turner, D. W.; Andrews, R. L.; Siegmund, C. W. *AIChE Symp. Ser*. **1972**, *68*, No. 126, 55.

(5) Dean, A. M.; Hardy, J. E.; Lyon, R. K. *Thermal DeNOx, 19th Symp. (Int.) Combust. Proc.*; The Combustion Institute: Pittsburgh, PA, 1982.

(6) Perry, R. A.; Steibers, D. L. *Nature* **1986**, *324*, 657.

(7) Snyder, L. R., *Anal. Chem*. **1969**, *41*, 314.

(8) Brandenburg, C. F.; Latham, D. R. *J. Chem. Eng. Data* **1968**, *13*, 391.

(9) Lifshitz, A.; Tamburn, C.; Suslensky, A. *J. Phys. Chem*. **1989**, *93*, 4099.

(10) Mackie, J. C.; Colket, M. B.; Nelson, P. F.; Esler, M. *Int. J. Chem. Kinet*. **1991**, *23*, 733.

(11) Mackie, J. C.; Colket, M. B.; Nelson, P. F. *J. Phys. Chem*. **1990**, *94*, 4099.

(12) Morris, V. R.; Bhatia, S. C.; Stelson, A.; Hall, J. H., Jr. *Energy & Fuels* **1991**, *5*, 126.

(13) Ruhemann, S. *Braunkohle* **1929**, *28*, 749.

(14) Dubnikova, F.; Lifshitz, A. *J. Phys. Chem*. **1998**, *102*, 10 880.

(15) Martoprawiro, M.; Bacskay, G. B.; Mackie, J. C. *J. Phys. Chem*. **1999**, *103*, 3923.

(16) Zhai, L.; Zhou, X.; Liu, R. *J. Phys. Chem*. **1999**, *103*, 3917.

(17) Halgren, T.; Lipscomb, W. *J. Chem. Phys*. **1973**, *58*, 1569.

(18) Kikuchi, O.; Hondo, Y.; Morihashi, K.; Nakayama, M. *Bull. Chem. Soc. Jpn*. **1988**, *61*, 291.

(19) Laskin, A.; Lifshitz, A. *J. Phys. Chem*. **1998**, *102*, 928.

(20) Rao, V. S.; Skinner, G. B. *J. Phys. Chem*. **1984**, *88*, 5990. Rao, V. S.; Skinner, G. B. *J. Phys. Chem*. **1984**, *92*, 2442.

(21) Kiefer, J. H.; Mizerka, L. J.; Patel, M. R.; Wei, H.-C. *J. Phys. Chem*. **1985**, *89*, 2013.

(22) Braun-Unkoff, M.; Frank, P.; Just, T. *22nd Symp. (Int.) Combust. Proc.*; The Combustion Institute: Pittsburgh, PA, 1988; p 1053.

(23) Madden, L. K.; Moskaleva, L. V.; Kristyan, S.; Lin, M. C. *J. Phys. Chem*. **1997**, *101*, 6790.

(24) Dubnikova, F.; Lifshitz, A. *J. Phys. Chem. A* **1998**, *102*, 10 880. Dubnikova, F.; Lifshitz, A. *J. Phys. Chem. A* **2000**, *104*, 530.

(25) Gaussian 94, Revision B.1; Frisch, M. J.; Trucks, G. W.; Schlegel, H. B.; Gill, P. M. W.; Johnson, B. G.; Robb, M. A.; Cheeseman, J. R.; Keith, T.; Petersson, G. A.; Montgomery, J. A.; Raghavachari, K.; Al-Laham, M. A.; Zakrzewski, V. G.; Ortiz, J. V.; Foresman, J. B.; Cioslowski, J.; Stefanov, B. B.; Nanayakkara, A.; Challacombe, M.; Peng, C. Y.; Ayala, P. Y.; Chen, W.; Wong, M. W.; Andres, J. L.; Replogle, E. S.; Gomperts, R.; Martin, R. L.; Fox, D. J.; Binkley, J. S.; Defrees, D. J.; Baker, J.; Stewart, J. P.; Head-Gordon, M.; Gonzalez, C.; Pople, J. A. Gaussian, Inc.: Pittsburgh, PA, 1995.

(26) Jones, J.; Bacskay, G. B.; Mackie, J. C.; Doughty, A. *J. Chem. Soc., Faraday Trans*. **1995**, *91*, 1587.

(27) Leidreiter, H. I.; Wagner, H. Gg. *Z. Phys. Chem. N. F*. **1987**, *153*, 99.

(28) Nam, H.-H.; Leroi, G. E.; Harrison, J. F. *J. Phys. Chem*. **1991**, *95*, 6514.

(29) Liu, R.; Tate, D. R.; Clark, J. A.; Moody, P. R.; VanBuren, A. S.; Krauser, J. A. *J. Phys. Chem*. **1996**, *100*, 3430.

(30) August, T.; Kroto, H. W.; McNaughton, D.; Phillips, K.; Walton, D. R. M. *J. Mol. Spectrosc.* **1988**, *130*, 424.

(31) Terentis, A.; Doughhty, A.; Mackie, J. C. *J. Phys. Chem*. **1992**, *96*, 10 334.

(32) Ikeda, E.; Mackie, J. C. *J. Anal. Appl. Pyrolysis* **1995**, *34*, 47.